Technical Note

Shear Strength Behavior of Soils Reinforced with Weak Fibers

Chunling Li, M.ASCE[1]; and Jorge G. Zornberg, F.ASCE[2]

Abstract: Soils reinforced with randomly distributed fibers will have higher shear strength and improved mechanical properties compared to unreinforced soil. Most of the previous research on fiber reinforcement focused on the behavior when the governing mode of failure is the pullout of fibers from a fiber matrix. In recent years, fibers with relatively low tensile strength (e.g., fibers made from recycled products or natural plant fibers) have been considered for soil reinforcement, but their mechanical response has not been studied extensively. In this paper, an experimental testing program is conducted using intentionally selected weak fibers (paper strip). The intention is not to demonstrate the usage of paper fibers as a reinforcement material, but to study the stress-strain behavior and shear strength envelope of fiber-reinforced soil when the governing mode of failure is fiber breakage. **DOI: 10.1061/(ASCE)GT.1943-5606.0002109.** © *2019 American Society of Civil Engineers.*

Author keywords: Fiber reinforcement; Tension; Breakage; Pullout; Shear strength.

Downloaded from ascelibrary.org by University of Texas at Austin on 10/03/19. Copyright ASCE. For personal use only; all rights reserved.

Introduction

Fiber reinforcement is considered a promising ground reinforcement technique in projects involving slope stabilization, embankment construction, subgrade stabilization, and stabilization of thin veneers such as landfill covers. Soils reinforced with randomly distributed short discrete fibers were found to have higher shear strength and improved mechanical properties such as higher resistance to cracking and erosion (e.g., Tang et al. 2012).

Many researchers have studied the shear strength envelopes of fiber-reinforced soil, considering the fiber/soil mixture as a composite material. The general findings are that fiber reinforcement increases the peak shear strength of soil, limits postpeak strength loss, and changes the soil behavior to a more ductile one (e.g., Gray and Ohashi 1983; Zornberg 2002; Yetimoglu and Salbas 2003; Consoli et al. 2007; Li and Zornberg 2013). The shear strength envelope of fiber-reinforced soil has been reported to be bilinear by many researchers (e.g., Gray and Ohashi 1983). According to the discrete framework proposed by Zornberg (2002), the shear strength envelope of fiber-reinforced soil includes two sections: (1) at low confining pressure where the friction angle of fiber-reinforced soil shows increase over that of unreinforced soil and (2) at higher confining pressures where the failure envelope shows a higher cohesion intercept but a friction angle similar to that of unreinforced soil. The break on the bilinear shear strength envelope is identified as the critical confining pressure, and it corresponds to the confining pressure at which the failure mode changes from the pullout of fiber from soil matrix to the tensile yielding of the fibers. Based on this assumption, an analytical expression of the critical confining pressure was derived (Zornberg 2002). A similar concept was also identified in other analytical models (Michalowski and Zhao 1996; Michalowski and Čermák 2003). Consoli et al. (2007) reported a bilinear shear strength envelope for sand reinforced with extensible fibers that yielded during triaxial tests. Other researchers reported bilinear or curvilinear shear strength envelopes for fiber-reinforced soil, even though fiber breakage or yielding was not observed (Nataraj and McManis 1997; Maher and Gray 1990).

For the commonly used polymeric fibers available commercially, the failure mode under confining pressures typical of geotechnical projects is fiber pullout because of the relatively high tensile strength and short length of the fibers. In recent years, materials with relatively low tensile strength [e.g., shredded carpet (Wang 1999) or natural plant fibers (Sivakumar Babu and Vasudevan 2008; Prabakar and Sridhar 2002)] have been considered for use as potential reinforcement inclusions. The mechanical response for fiber-reinforced soil when fiber breakage is the governing failure mode has not been widely studied.

The main purpose of this paper is to evaluate the behaviors of fiber-reinforced soil when the governing failure mode is tensile breakage. For this research, paper fibers, which have relatively low tensile strength, were used in a testing program to study fiber breakage failure under representative confining pressures. Paper is not a realistic fiber material to use in the field owing to its low strength and weakening by moisture. The dimension of paper fibers used in this study is different from those of typical fibers. However, to investigate the effect of fiber breakage on the behavior of fiber-reinforced soil, the use of paper as a weaker fiber has some research value. Stress-strain behavior, shear strength envelope, and the prediction of critical confining pressure were evaluated. The purpose of this study is not to demonstrate the use of paper fiber as reinforcement but to use intentionally selected weak fibers to improve the understanding of fiber-reinforced soil behavior when fiber breaks. The results from this study may provide opportunities for design optimization of fiber reinforcement to be used in future applications.

Summary of Discrete Framework

Zornberg (2002) proposed a discrete framework for predicting the shear strength of a fiber/soil mixture based on discrete characteristics

[1]Senior Geotechnical Engineer, Soil and Land Use Technology, Inc., 530 McCormick Dr. Suite S, Glen Burnie, MD 21061 (corresponding author). ORCID: https://orcid.org/0000-0003-4084-9642. Email: cli@salutinc.com

[2]Professor and W. J. Murray, Jr. Fellow in Engineering, Dept. of Civil, Architectural and Environmental Engineering, Univ. of Texas at Austin, Austin, TX 78712.

Note. This manuscript was submitted on May 1, 2018; approved on March 15, 2019; published online on June 26, 2019. Discussion period open until November 26, 2019; separate discussions must be submitted for individual papers. This technical note is part of the ***Journal of Geotechnical and Geoenvironmental Engineering***, © ASCE, ISSN 1090-0241.

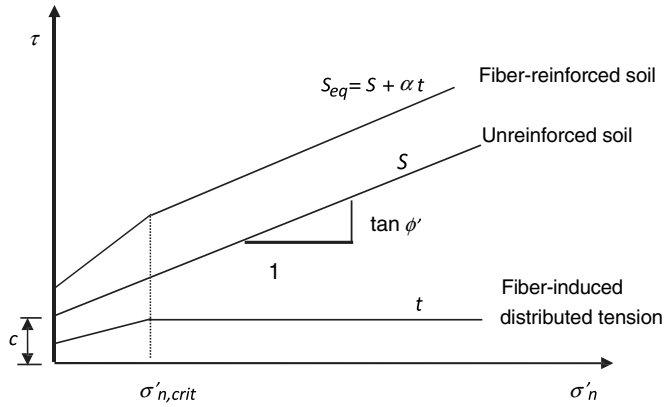

Fig. 1. Representation of equivalent shear strength according to discrete framework.

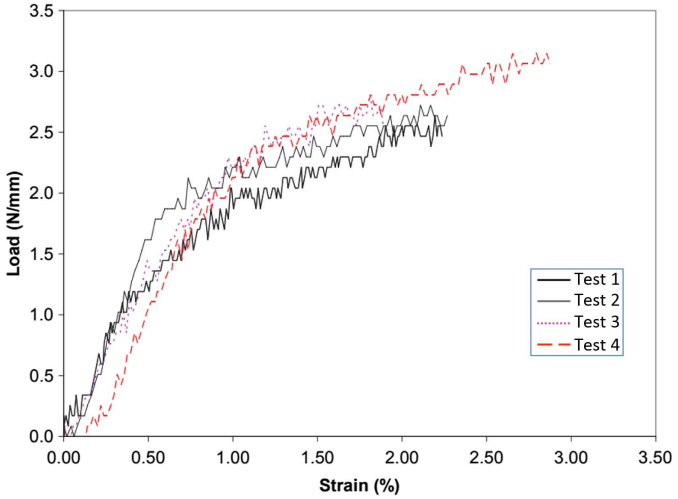

Fig. 2. Tensile strength test result of paper fiber (fibers cut along width direction of paper sheet).

of fibers and soils. In this discrete framework, the mechanism of fiber reinforcement was considered to be attributable to a distributed tension by the fibers within the soil matrix. The distributed tension is governed either by the pullout resistance of fibers under low confining pressures or by the tensile strength of fibers under high confining pressure. The change of failure mechanism from fiber pullout to tensile breakage occurs at a critical confining pressure, at which the pullout resistance equals the tensile strength. A bilinear shear strength envelope, as shown in Fig. 1, was proposed for fiber-reinforced soil, which included a segment with increased friction angle and cohesion intercept (below the critical confining pressure) and a segment with increased cohesion intercept only (above the critical confining pressure).

Experimental Testing Program

The behaviors of fiber-reinforced soil under pullout failure mode have been widely studied by many researchers (Gray and Ohashi 1983; Gray and Al-Refeai 1986; Zornberg 2002; Li and Zornberg 2013; Tang et al. 2007). For this study, intentionally selected low-tensile-strength fibers were used in a triaxial testing program to study the behavior of fiber-reinforced soil when the governing failure mode is fiber breakage. The fibers used in this research were cut from commercially available printing paper with a width of 8.73 mm and two different lengths (108 and 54 mm). They were cut from a sheet of paper along the direction of width or the direction of length. The dry mass of the paper was 18 g/sheet. A tensile testing program was conducted to study the tensile strength of the material. The samples used in the tensile tests had a width of 25.4 mm (1 in.) and a gauge length of 203.2 mm (8 in.). The samples were loaded using a universal testing machine at a strain rate of 2.5 mm/min. Fig. 2 shows the stress-strain behavior of the paper fibers as observed in the tensile test. The average tensile strength of the fiber material found was 2.83 N/mm.

The fibers used in three series of the triaxial tests (Series A, B, and C) were 108, 54, and 54 mm long, respectively, and were placed at volumetric contents of 0.23%, 0.46%, and 0.23%, respectively. The soil used in this research was a clean sand classified as SP (uniform sand) according to the Unified Soil Classification System (USCS). The geotechnical properties of this soil are listed in Table 1.

To prepare the specimen for triaxial testing, the weighted soil and desired amount of fibers were thoroughly mixed by hand until visual inspection showed homogeneous fiber distribution. The mixture was then transferred into a rubber membrane–wrapped mold. A vibrating table was used to compact the sand/fiber mixture to a dry unit weight of 15.4 kN/m^3, which corresponds to approximately 48% of relative density. The prepared specimen had a diameter of 152 mm and a height of 304 mm. The prepared specimens were tested in dry conditions in a large-scale triaxial chamber. The drainage valve of triaxial specimen was opened to air, which led to testing conditions similar to those of a consolidated drained test. A rate of 2 mm/min was used for the loading process. The confining pressures used in this testing program ranged from 21 to 738 kPa. The number of broken fibers within each specimen was quantified after the completion of each test. Table 2 shows the scope of the tests.

Table 1. Mechanical properties of soil used

Property	Value
Relative density, D_r (%)	48
Dry unit weight, γ_d (kN/m^3)	15.54
Effective friction angle, ϕ' (degrees)	31.6
Effective cohesion, c' (kPa)	0
USCS	SP
Percentage of fines by weight (%)	≤1
Average diameter, d_{50} (mm)	0.7
Maximum void ratio, e_{max}	0.76
Minimum void ratio, e_{max}	0.56
Coefficient of uniformity, C_u	1.8
Coefficient of curvature, C_c	1.0

Stress-Strain Relationship of Paper Fiber/Soil Mixture

The stress-strain curves obtained for specimens reinforced with paper fibers are shown in Fig. 3. The tests shown in the figure were conducted under confining pressures of 60 and 490 kPa. Unlike the specimens reinforced using polymeric fibers, the specimens reinforced using paper fibers show a well-defined postpeak shear strength loss. This is because the tension developed within the paper fibers cannot be maintained once the fiber breaks. The specimen tested under 60 kPa still shows an improved residual strength,

Downloaded from ascelibrary.org by University of Texas at Austin on 10/03/19. Copyright ASCE. For personal use only; all rights reserved.

Table 2. Scope of experimental testing program

Series	Number of tests	Test conditions	Soil: USCS classification	Soil: Density D_r (%)	Soil: Density γ_d (kN/m^3)	Fibers: Fibers	Fibers: Length, l_f (mm)	Fibers: Fiber content, χ (% by volume)
A	6	Triaxial compression, dry specimen, CD	SP	48	15.54	Weak fiber inclusions	108	0.23
B	6						54	0.46
C	3						54	0.23

Note: CD = consolidated drained.

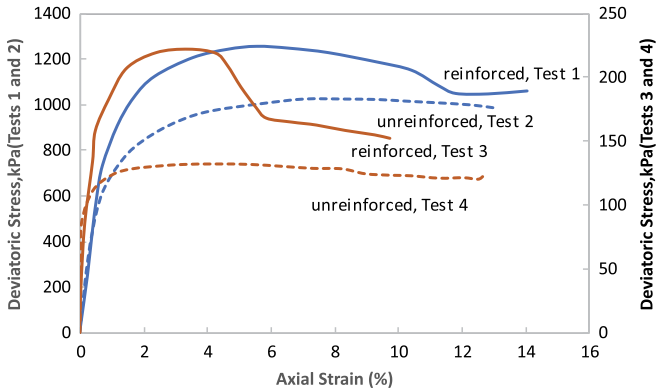

Fig. 3. Stress-strain behavior of specimens reinforced using paper fibers (Series A). Tests 1 and 2: $\sigma_3 = 490$ kPa; Tests 3 and 4: $\sigma_3 = 60$ kPa; reinforcement: 0.23% 108-mm paper fibers. Specimen reinforced using 108-mm-long fibers were not tested under confining pressure of 735 kPa.

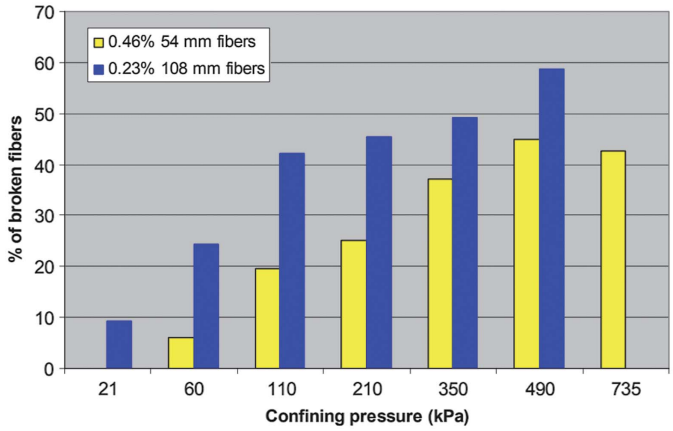

Fig. 4. Percentage of broken fibers observed after each test.

while approximately the same residual shear strength as for unreinforced specimens was observed in tests conducted under confining pressure of 490 kPa. That is, the postpeak shear strength loss becomes more significant under a higher confining pressure level. Of all the specimens tested, approximately one-third of the specimens (mostly under relatively high confining pressures) showed localized shear band after the tests. The other specimens showed a bulging drumlike shape after the tests. However, the stress-strain responses for both failed shapes show no distinct difference.

The number of broken fibers was counted after the triaxial tests, and the percentages of broken fibers are shown in Fig. 4. As shown in Fig. 4, the percentage of broken fibers was higher under higher confining pressures. Some of the fibers were found to have broken into more than two pieces at high confining pressures. According to Zornberg (2002), the areal percentage of fibers intersecting a failure plane for randomly distributed fibers can be approximated by the volumetric fiber content. Based on that, it was estimated that approximately 18% or 36% fibers would intersect a failure plane for volume metric fiber content of 0.23% and 0.46%, respectively. It is noted that the percentage of broken fibers from Fig. 4 is above the theoretical percentage of fibers intersecting a failure plane for some of the tests. This is understandable because the fibers away from the shear band (if it forms) are also subject to the stresses induced by the loads and may develop tension . However, the shear strength of fiber-reinforced soil should only be affected by those intersecting the failure plane, considering force equilibrium on the failure plane.

For the range of confining pressures used in this study, the fibers in the triaxial tests exhibited two failure modes: fiber pullout and fiber breakage. As illustrated in the section "Prediction Of Critical Confining Pressure," the pullout failure mode was more significant under low confining pressures and the fiber breakage was more pronounced under high confining pressures. The improved postpeak response over unreinforced soil under low confining pressure could be attributed to the contribution of those fibers subjected to pullout failure, which could be maintained even after the pullout resistance of the fibers was achieved. At high confining pressure when the governing failure mode was fiber breakage, the residual strength of the fiber-reinforced specimen dropped to that of the unreinforced specimen after all the fibers intersecting the shear band broke. After the fibers broke, tension might still have developed within the broken fibers, but their contribution to the shear strength would be lost gradually, as evidenced by the fact that the postpeak shear strength of fiber-reinforced soil was essentially the same as unreinforced soil under relatively high confining pressures.

Prediction of Critical Confining Pressure

Results obtained from Series A and B were used to validate the prediction of critical confining pressure. Specimens for Series A were prepared using 0.23% (by volume), 108-mm-long paper fibers as reinforcement, while specimens for Series B were prepared using 0.46%, 54-mm-long paper fibers. The percentage of broken fibers after the completion of each test is shown in Fig. 4. The results show that the percentage of broken fibers increases with increasing confining pressure. However, the percentage of broken fibers appears to reach a relatively constant value at high confining pressures.

For randomly distributed fibers intersecting the failure plane, the embedment lengths of these fibers range from 0 to half-length. It is expected that the fibers with the largest embedment length will break first under low confining pressures. Those fibers with smaller embedment lengths will require a higher confining pressure to break. Inspection of broken fibers shows that for specimens prepared using 108-mm-long fibers, fibers broke approximately at midlength under a confining pressure of 21 kPa. An increased

Downloaded from ascelibrary.org by University of Texas at Austin on 10/03/19. Copyright ASCE. For personal use only; all rights reserved.

number of fibers with shorter embedment length than half-length was found to break at a higher confining pressure, 210 kPa.

The relationship between the embedment length and critical confining pressure is evaluated in what follows. For fibers that break in tension, the pullout resistance should be greater than the tensile strength of fibers. The normal stress that should be exceeded for an individual fiber to break is as follows:

$$\sigma'_{n,f} \geq \frac{\sigma_{f,ult} - 4\left(\frac{l_e}{df}\right) c_{i,c\cdot c'}}{4\left(\frac{l_e}{df}\right) c_{i,\phi\cdot \tan\phi'}} \tag{1}$$

where $\sigma'_{n,f}$ = normal stress acting on fiber surface; $\sigma_{f,ult}$ = ultimate tensile strength of fibers; l_e = fiber embedment length; c' = cohesion intercept of unreinforced soil; ϕ' = friction angle of unreinforced soil; d_f = diameter of fibers; $c_{i,c}$ = coefficient of interaction for adhesion (= adhesion of fiber–soil interface/cohesion intercept of soil); and $c_{i,\phi}$ = coefficient of interaction for friction angle (= $\tan\delta/\tan\phi$, δ = interface friction angle). The interface shear strength between fibers and soil may be tested by pulling a long uncut fiber embedded in soil (Li 2005; Tang et al. 2010). $C_{i,c}$, and $C_{i,\phi}$ values may be assumed based on similar geotextile–soil interface shear strength results as a preliminary estimate if no fiber–soil interface shear strength test data are available.

As mentioned earlier, the embedment length of random fibers ranges from 0 to half the fiber length (l_f) and average one-fourth of l_f. For randomly distributed fibers, the average of $\sigma_{n,f}$, (defined as $\sigma_{n,ave}$) can be assumed to equal the normal stress acting on the failure plane of fiber-reinforced soil σ_n (i.e., $\sigma'_{n,ave} = \sigma'_n$) (Zornberg 2002). The lowest and average σn required for fiber to break, from Eqs. (2) and (3):

$$\min(\sigma'_{n,crit}) = \frac{\sigma_{f,ult} - 2\eta \cdot c_{i,c} \cdot c'}{2\eta \cdot c_{i,\phi} \cdot \tan\phi'} \tag{2}$$

$$\text{ave}(\sigma'_{n,crit}) = \frac{\sigma_{f,ult} - \eta \cdot c_{i,c} \cdot c'}{\eta \cdot c_{i,\phi} \cdot \tan\phi'} \tag{3}$$

where η is defined as the aspect ratio (= l_f/d_f). The following expression is used to determine the aspect ratio of fibers with a noncircular cross section:

$$\eta = \frac{A_{s,i}}{4A_{f,i}} \tag{4}$$

where $A_{s,i}$ = surface area of a single fiber; and $A_{f,i}$ = cross-sectional area of a single fiber. For paper fibers

$$\eta = \frac{b_f}{2T_f} \tag{5}$$

Eq. (3) is the same expression of critical confining pressure derived in the discrete framework (Zornberg 2002). The value calculated using Eq. (3) represents the most probable confinement at which the fiber breakage will take place. If c' equals zero, $\min(\sigma'_{n,crit})$ equals half of $\text{ave}(\sigma'_{n,crit})$.

Fibers with a shorter than average embedment length (i.e., $l_e \leq ¼\, l_f$) will break under a higher confining pressure than $\text{ave}(\sigma'_{n,crit})$. Theoretically, the confining pressure required for the number of broken fibers to reach the upper bound, $\max(\sigma'_{n,crit})$ is infinity, which corresponds to the case of $le = 0$. In practical terms, $\max(\sigma'_{n,crit})$ corresponds to the confining pressure beyond which the failure is governed by fiber breakage. The $\max(\sigma'_{n,crit})$ determined from the shear strength envelope is approximately five to six times the $\min(\sigma'_{n,crit})$. It is expected that both modes of failure (fiber breakage and fiber pullout) will take place for normal stresses between $\min(\sigma'_{n,crit})$ and $\max(\sigma'_{n,crit})$. The number of broken fibers should be smaller than the number of fibers acting in tension.

The $\sigma'_{n,crit}$ obtained from Eq. (2) or (3) corresponds to the average normal stress at the fiber–soil interface. This has been assumed to equal the normal stress acting on the failure plane of the fiber-reinforced specimen (Zornberg 2002). It should be noted that the normal stress acting on the failure plane is not the same as the confining stress in a triaxial test setup. To compare the $\sigma'_{n,crit}$ derived from Eqs. (2) and (3) with experimental results, the corresponding minor principal stress (or confining pressure in triaxial compression tests), $\sigma'_{3,crit}$, can be calculated using the relationship between σ'_3 and σ'_n as follows:

$$\sigma'_3 = \sigma'_n\left[\tan\phi'_{eq}\left(\tan\phi'_{eq} - \frac{1}{\cos\phi'_{eq}}\right) + 1\right] + c'\left(\tan\phi'_{eq} - \frac{1}{\cos\phi'_{eq}}\right) \tag{6}$$

Prediction of the critical confinement can be verified using the experimental results obtained in this investigation. For the 108-mm-long paper fibers used, the aspect ratio calculated from the foregoing expression is $\eta = 508$. Accordingly, $\min(\sigma'_{n,crit})$ and $\min(\sigma'_{3,crit})$ are estimated to be 43.2 and 25.4 kPa using Eqs. (2) and (3), respectively. Although the lowest confining pressure at which the breakage of fibers initiates cannot be determined precisely because of the limited number of tests, an approximate value of $\min(\sigma_{3,crit})$ can be inferred from the lowest confining pressure at which broken fibers were identified. Of the 108-mm-long fibers, 9% broke in tension in tests conducted using a confining pressure of 21 kPa. This confining pressure is close to the predicted value of $\min(\sigma'_{3,crit})$.

For the 54-mm-long fibers, the value of min $(\sigma'_{n,crit})$ calculated from Eq. (2) is 86.2 kPa, which corresponds to a $\min(\sigma'_{3,crit})$ of 55.2 kPa using Eq. (6). The test conducted using a confining pressure of 60 kPa led to 6% broken fibers. No fiber breakage was identified in the test conducted under a confining pressure of 21 kPa. Consequently, $\min(\sigma'_{3,crit})$ is expected to be below 60 kPa. These test results indicate that Eq. (2) gives a reasonable prediction of the lowest confining pressure at which fiber breakage initiates.

Shear Strength Envelope under Fiber Breakage Failure Mode

An analytical expression of equivalent shear strength for fiber breakage failure mode is derived in the discrete framework (Zornberg 2002). The suitability of relationships is evaluated in this section.

The shear strength envelope obtained from Series A is shown in Fig. 5. The specimens in this series were placed at $\chi = 0.23\%$ using 108-mm-long paper fibers. Confining pressures ranging from 21 to 490 kPa were used in the test. The nonlinear shear strength envelope was fitted using three straight-line sections. Fig. 5 compares the experimental shear strength envelope with that predicted by the discrete framework. As shown in the figure, fiber-reinforced soil shows an increased friction angle under low confining pressures. On the other hand, an increased cohesion intercept with approximately the same friction angle as the unreinforced soil is observed under high confining pressures. These observations are consistent with the response predicted by the discrete framework. Overall, good agreement can be observed between the predicted shear strength and experimental results for the case of low

Downloaded from ascelibrary.org by University of Texas at Austin on 10/03/19. Copyright ASCE. For personal use only; all rights reserved.

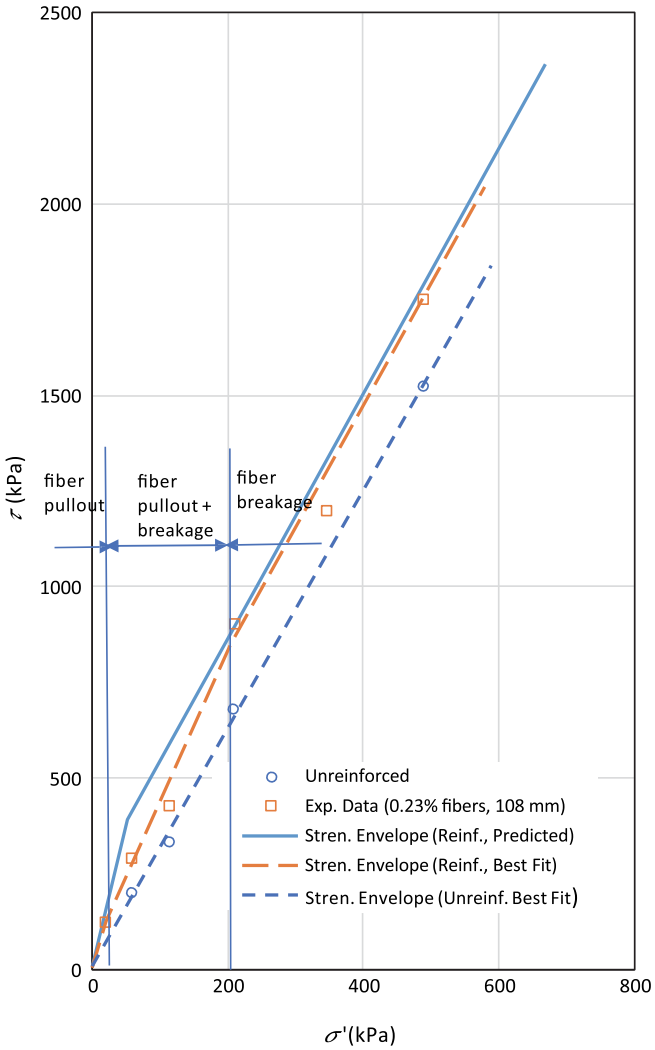

Fig. 5. Comparison of predicted and experimental shear strength results obtained from Series A ($\chi = 0.23\%$, $l_f = 108$ mm).

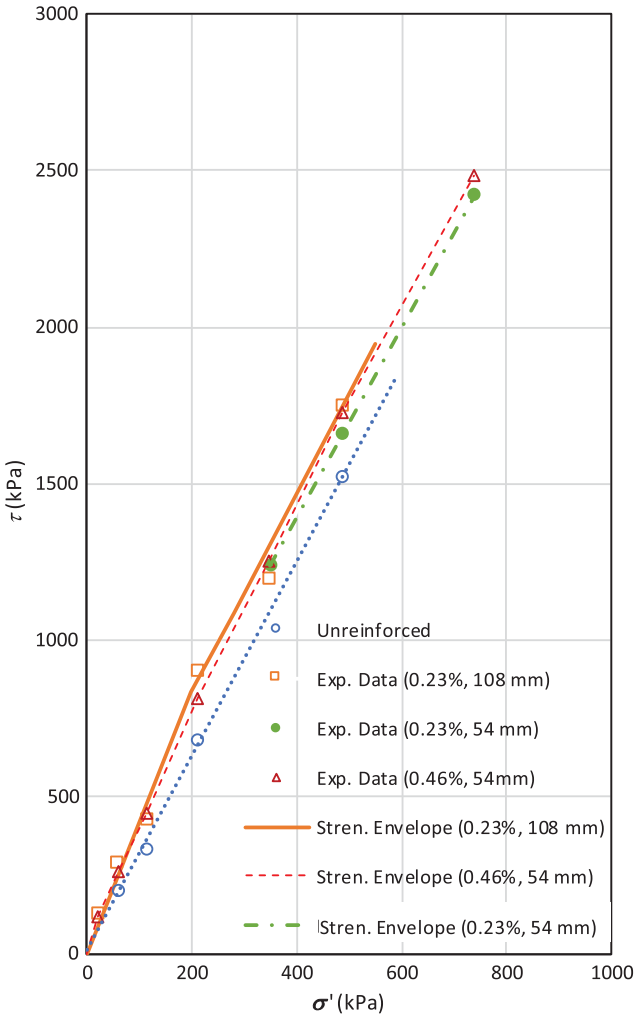

Fig. 6. Comparison between shear strength results for specimens reinforced with 0.23%, 108-mm fibers; 0.46%, 54-mm fibers, and 0.23%, 54-mm fibers.

confining pressures and for high confining pressures. That is, the discrete framework gives a reasonable prediction of the equivalent shear strength if the failure mode is purely by fiber pullout or by breakage. However, for confining pressures in the vicinity of the predicted ave($\sigma'_{n,crit}$) (i.e., where both modes of failure take place), the shear strength envelope shows a smooth transition zone rather than a sharp break at the critical confining pressure as idealized by the discrete framework.

According to the discrete framework (Zornberg 2002), under low confining pressure when failure is governed by fiber pullout, the equivalent shear strength is governed by the product of fiber content and aspect ratio ($\chi \cdot \eta$). Under high confining pressure when failure is governed by fiber breakage, the equivalent shear strength is a function of fiber content (χ) but is independent of fiber aspect ratio (η). The sensitivity of equivalent shear strength to fiber content and aspect ratio for soils reinforced with paper fibers is also examined. Tests on Series B and C were conducted in addition to those on Series A to verify the analytical expressions of equivalent shear strength defined by the discrete framework (Zornberg 2002). The volumetric fiber content (χ) selected in Series B was 0.46% and the length of fibers was 54 mm. This gives the same value of ($\chi \cdot \eta$) as in Series A. The fibers used in Series C were also 54 mm long. However, the fiber content selected in Series C was 0.23%, which is half the fiber content used in Series B. The shear strength results of Series A, B, and C are presented in Fig. 6.

The results obtained from Series B and Series C (Fig. 6) show that for the same fiber length, the increase in the equivalent shear strength under high confining pressure is approximately proportional to the fiber content with the shear strength of fiber-reinforced soil being parallel to the unreinforced shear strength envelope. This observation is consistent with the prediction of the discrete framework.

For specimens prepared using a constant value of ($\chi \cdot \eta$), the shear strength envelopes obtained from Series A and B are approximately the same under low confining pressures, which is also consistent with the discrete framework. Under high confining pressure when the failure is governed by the breakage of fibers, the shear strength envelopes obtained from Series A and B are found to be similar, which is different from the prediction by the discrete framework (Zornberg 2002).

A comparison of the results obtained from Series A and C shows that the shear strength envelope under high confining pressure is also dependent on the aspect ratio (Fig. 6). With the same fiber content used, specimens prepared using 108-mm-long fibers in Series A are found to have a higher shear strength than specimens

Downloaded from ascelibrary.org by University of Texas at Austin on 10/03/19. Copyright ASCE. For personal use only; all rights reserved.

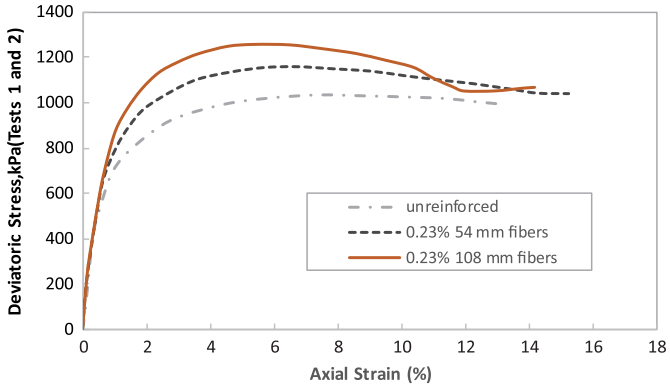

Fig. 7. Comparison of stress-strain curves of specimens prepared using same fiber contents at different aspect ratios.

prepared using 54-mm-long fibers when the failure is governed by the breakage failure mode. This is inconsistent with the discrete framework (Zornberg 2002). Such inconsistency can be attributed to the stress-strain behavior of the paper fibers, unlike what was assumed in the discrete framework. Plastic yielding was assumed in the discrete framework when the tension within fiber reached the maximum tensile strength. However, the paper fiber used in this study showed brittle rupture behavior when the tensile strength is reached. The individual fibers within the fiber-reinforced specimen could reach tensile strength at a different strain level. As the fiber breaks, the tension within the fibers cannot be maintained. Consequently, the average tension within individual fibers at a given strain level is smaller than their tensile strength. If breakage of individual fibers takes place within a narrow range of strains, the stress-strain curve is expected to show a high peak strength but also a steep postpeak strength loss. In contrast, if the breakage of fibers takes place in a wide range of strain, the stress-strain curve will show a low peak shear strength and a flatter postpeak portion.

Fig. 7 compares the stress-strain behavior of specimens reinforced using same fiber content (0.23% by volume) but different fiber lengths (54 and 108 mm). The tests were conducted under a confining pressure of 490 kPa, which is beyond the predicted $\sigma_{n,crit}$. The specimen reinforced using longer fibers shows higher peak strength, but a more significant postpeak shear strength loss with increasing strain. This shows that the fibers break within a narrower range of strains in specimens reinforced with long fibers, which is closer to the assumptions of the discrete framework (i.e., all fiber tensile strength is mobilized at peak strength). Therefore, the predicted equivalent shear strength envelope is more accurate for soils reinforced using longer fibers.

Summary

The behavior of fiber-reinforced soil for conditions leading to breakage of fibers was investigated in this paper. The experimental testing program included triaxial compression tests on soils reinforced using fibers with a low tensile strength (paper fiber). The following conclusions can be drawn from this investigation:

1. The presence of two failure modes (fiber pullout and fiber breakage) that define the equivalent shear strength of fiber-reinforced soil, as identified by the discrete framework (Zornberg 2002), was observed in this study.
2. The shear strength envelope of fiber-reinforced soil does not show a sharp break at the critical confining pressure, as indicated by the discrete framework (Zornberg 2002). Both types of failure mode (fiber breakage and fiber pullout) take place within a certain range in the vicinity of the critical confining pressure. The minimum and average critical confining pressure at which the breakage of random fibers initiates can be predicted using the revised equations from this study.
3. The effects of fiber content and aspect ratio on the equivalent shear strength under fiber breakage failure mode was examined. For the paper fibers used in this study, soil reinforced using longer fibers was found to have a higher shear strength than soil reinforced using shorter fibers at a given fiber content. The equivalent shear strength predicted by the discrete framework is a good approximation of the test results obtained for specimens reinforced with longer fibers.

References

Consoli, N. C., K. S. Heineck, M. D. T. Casagrande, and M. R. Coop. 2007. "Shear strength behavior of fiber-reinforced sand considering triaxial tests under distinct stress paths." *J. Geotech. Geoenviron. Eng.* 133 (11): 1466–1469. https://doi.org/10.1061/(ASCE)1090-0241(2007)133:11(1466).

Gray, D. H., and T. Al-Refeai. 1986. "Behavior of fabric-versus fiber-reinforced sand." *J. Geotech. Eng.* 112 (8): 804–820. https://doi.org/10.1061/(ASCE)0733-9410(1986)112:8(804).

Gray, D. H., and H. Ohashi. 1983. "Mechanics of fiber-reinforcement in sand." *J. Geotech. Eng.* 109 (3): 335–353. https://doi.org/10.1061/(ASCE)0733-9410(1983)109:3(335).

Li, C. 2005. *Mechanical response of fiber-reinforced soil*. Ph.D. dissertation, Dept. of Civil, Architectural and Environmental Engineering, Univ. of Texas at Austin.

Li, C., and J. G. Zornberg. 2013. "Mobilization of reinforcement forces in fiber-reinforced soil." *J. Geotech. Geoenviron. Eng.* 139 (1): 107–115. https://doi.org/10.1061/(ASCE)GT.1943-5606.0000745.

Maher, M. H., and D. H. Gray. 1990. "Static response of sand reinforced with randomly distributed fibers." *J. Geotech. Eng.* 116 (11): 1661–1677. https://doi.org/10.1061/(ASCE)0733-9410(1990)116:11(1661).

Michalowski, R. L., and J. Čermák. 2003. "Triaxial compression of sand reinforced with fibers." *J. Geotech. Geoenviron. Eng.* 129 (2): 125–136. https://doi.org/10.1061/(ASCE)1090-0241(2003)129:2(125).

Michalowski, R. L., and A. G. Zhao. 1996. "Failure of fiber-reinforced granular soils." *J. Geotech. Eng.* 122 (3): 226–234. https://doi.org/10.1061/(ASCE)0733-9410(1996)122:3(226).

Nataraj, M. S., and K. L. McManis. 1997. "Strength and deformation properties of soils reinforced with fibrillated fibers." *Geosynthetics Int.* 4 (1): 65–79. https://doi.org/10.1680/gein.4.0089.

Prabakar, J., and R. S. Sridhar. 2002. "Effect of random inclusion of sisal fibre on strength behaviour of soil." *Constr. Build. Mater.* 16 (2): 123–131. https://doi.org/10.1016/S0950-0618(02)00008-9.

Sivakumar Babu, G. L., and A. K. Vasudevan. 2008. "Strength and stiffness response of coir fiber-reinforced tropical soil." *J. Mater. Civ. Eng.* 20 (9): 571–577. https://doi.org/10.1061/(ASCE)0899-1561(2008)20:9(571).

Tang, C., B. Shi, W. Gao, F. Chen, and Y. Cai. 2007. "Strength and mechanical behavior of short polypropylene fiber reinforced and cement stabilized clayey soil." *Geotext. Geomembr.* 25 (3): 194–202. https://doi.org/10.1016/j.geotexmem.2006.11.002.

Tang, C. S., B. Shi, Y. J. Cui, C. Liu, and K. Gu. 2012. "Desiccation cracking behavior of polypropylene fiber-reinforced clayey soil." *Can. Geotech. J.* 49 (9): 1088–1101. https://doi.org/10.1139/t2012-067.

Tang, C. S., B. Shi, and L. Z. Zhao. 2010. "Interfacial shear strength of fiber reinforced soil." *Geotext. Geomembr.* 28 (1): 54–62. https://doi.org/10.1016/j.geotexmem.2009.10.001.

Downloaded from ascelibrary.org by University of Texas at Austin on 10/03/19. Copyright ASCE. For personal use only; all rights reserved.

Wang, Y. 1999. "Utilization of recycled carpet waste fibers for reinforcement of concrete and soil." *Polym. Plast. Technol. Eng.* 38 (3): 533–546. https://doi.org/10.1080/03602559909351598.

Yetimoglu, T., and O. Salbas 2003. "A study on shear strength of sands reinforced with randomly distributed discrete fibers." *Geotext. Geomembr.* 21 (2): 103–110. https://doi.org/10.1016/S0266-1144(03)00003-7.

Zornberg, J. G. 2002. "Discrete framework for limit equilibrium analysis of fiber- reinforced soil." *Géotechnique* 52 (8): 593–604. https://doi.org/10.1680/geot.2002.52.8.593.

Downloaded from ascelibrary.org by University of Texas at Austin on 10/03/19. Copyright ASCE. For personal use only; all rights reserved.